International Journal of Nanomedicine

Dovepress
open access to scientific and medical research

Open Access Full Text Article

ORIGINAL RESEARCH

Antibacterial activity of trimetal (CuZnFe) oxide nanoparticles

This article was published in the following Dove Press journal:
International Journal of Nanomedicine

Khalid E Alzahrani[1,2]
Abdurahman A Niazy[3]
Abdullah M Alswieleh[4]
Rizwan Wahab[5]
Ahmed M El-Toni[2]
Hamdan S Alghamdi[3]

[1]Department of Physics and Astronomy, King Saud University, Riyadh, Kingdom of Saudi Arabia; [2]King Abdullah Institute for Nanotechnology, King Saud University, Riyadh, Kingdom of Saudi Arabia; [3]Prince Naif Health Research Center, Molecular and Cell Biology Laboratory, College of Dentistry, King Saud University, Riyadh, Kingdom of Saudi Arabia; [4]Department of Chemistry, College of Science, King Saud University, Riyadh, Kingdom of Saudi Arabia; [5]Department of Zoology, College of Science, King Saud University, Riyadh, Kingdom of Saudi Arabia

Background: The increasing resistance of pathogenic bacteria to antibiotics is a challenging worldwide health problem that has led to the search for new and more efficient antibacterial agents. Nanotechnology has proven to be an effective tool for the fight against bacteria.

Methods: In this paper, we present the synthesis and traits of trimetal (CuZnFe) oxide nanoparticles (NPs) using X-ray diffraction, high-resolution transmission electron microscopy, and energy dispersive x-ray spectroscopy. We evaluated the antibacterial activity of these NPs against gram-negative *Escherichia coli* and gram-positive *Enterococcus faecalis* and then compared it to that of their pure single-metal oxide components CuO and ZnO.

Results: Our study showed that the antibacterial activity of the trimetal oxide NPs was greater against *E. coli* than against *E. faecalis*. Overall, the antimicrobial effect of trimetal NPs is between those of pure ZnO and CuO nanoparticles, which may mean that their cytotoxicity is also between that of pure ZnO and CuO NPs, making them potential antibiotics. However, the cytotoxicity of trimetal NPs to mammalian cells needs to be verified.

Conclusion: The combination of three metal oxide NPs (ZnO, CuO, and Fe_2O_3) in one multimetal (CuZnFe) oxide NPs will enhance the therapeutic strategy against a wide range of microbial infections. Bacteria are unlikely to develop resistance against this new NP because bacteria must go through a series of mutations to become resistant to the trimetal oxide NP. Therefore, this NP can combat existing and emerging bacterial infections.

Keywords: nanotechnology, antibacterial agents, nanoparticles, trimetal nanoparticles, *Escherichia coli*, *Enterococcus faecalis*

Introduction

Bacterial infections are major challenges for the medical field and have become a serious threat to human health and lives. An increasing number of species of bacteria have developed resistance against most common antibiotics from the misuse of these drugs.[1] The list of drug-resistant bacteria has increased dramatically, for example, *Enterobacter cloacae* is sulfonamide- and methicillin-resistant, *Staphylococcus aureus* is vancomycin-resistant, *Mycobacterium tuberculosis* is resistant to multiple drugs, and *Streptococcus pyogenes* and *Acinetobacter baumannii* are macrolide-resistant.[2–4] Generally, biofilm-growing bacteria are highly resistant to antibacterial drugs and the host immune system, although the exact mechanisms underlying such resistance are still not fully understood.[5,6] Biofilm is a structured community of bacteria embedded in a self-produced extracellular matrix of proteins, polysaccharides, and DNA. Consequently, infections involving biofilm formation are chronic and difficult to treat. Therefore, there is an urgent need to find alternative therapeutic approaches for overcoming the increasing resistance of bacteria to current antibiotics.

Correspondence: Khalid E Alzahrani
Department of Physics and Astronomy, King Abdullah Institute for Nanotechnology, King Saud University, PO Box 2455, Riyadh 11451, Kingdom of Saudi Arabia
Tel +966 55 300 1262
Email alzkhalid@ksu.edu.sa

Hamdan S Alghamdi
Molecular and Cell Biology Laboratory, College of Dentistry, King Saud University, PO Box 2455, Riyadh 11545, Kingdom of Saudi Arabia
Tel +966 50 341 8405
Email dalghamdi@ksu.edu.sa

submit your manuscript | www.dovepress.com
Dovepress
http://dx.doi.org/10.2147/IJN.S154218

Controlling the growth of bacterial biofilms using nanoparticles (NPs) has become the center of attention in the medical field. The use of NPs is a promising therapeutic strategy for overcoming the increasing emergence of multidrug-resistant bacteria. Although the antimicrobial effects of NPs have been verified using different types of NPs on various bacterial species, the bactericidal mechanisms of NPs are still being investigated. Several factors such as the physiochemical properties of NPs and the bacterial species involved might play important roles in the antibacterial activity of NPs. Some bacterial species are more sensitive to particular NPs than are others. Ag NPs are more efficient than Cu NPs against *Escherichia coli* and *S. aureus*, whereas *Bacillus subtilis* showed more susceptibility to Cu NPs than to Ag NPs.[7] Titanium dioxide NPs exhibited greater antibacterial activity against *E. coli* than against *Salmonella typhimurium*.[8] Dizaj et al[9] showed that Ag NPs have a greater antibacterial effect on *Streptococcus mutans* than do ZnO and Au NPs. The sensitivity of bacteria to NPs is related to the species whereby the cell structure of the bacteria influences its tolerance to NPs. Vancomycin-resistant bacteria (eg, *Enterococci*) develop an additional outer membrane that covers the cellular surface and protects the bacterium from the vancomycin. Vancomycin-capped Au NPs can penetrate the outer cell membrane, allowing the vancomycin to access the cellular surface.[10] Poly(vinyl alcohol)-coated ZnO NPs can kill bacterial cells by inducing oxidative stress.[11] Furthermore, the size of the NP plays an important role in its toxicity. Hayden et al[12] studied the effect of size reduction on the antibacterial efficiency of Au NPs and found that 2 nm Au NPs are more toxic to *B. subtilis* than 6 nm Au NPs.

Several types of metal and metal oxide NPs such as CuO, CaO, Ag and Ag_2O, Au, ZnO, and MgO have been investigated for their antibacterial effects. Diverse studies revealed that ZnO NPs exhibit a wide spectrum of antibacterial activities toward various gram-negative and gram-positive bacteria.[13] For example, they are very efficient at inhibiting the growth of gram-negative *E. coli* and *Pseudomonas aeruginosa* and gram-positive *S. aureus* and *B. subtilis*.[14–17] The antibacterial effect of ZnO NPs on *S. mutans* was compared with that of other NPs such as Ag and Au and it was observed that ZnO NPs had the lowest bactericidal activity.[18] However, many toothpastes contain Zn to combat dental plaque that is formed by bacteria such as *S. mutans*.[19] The antimicrobial activities of ZnO NPs have been found to be affected by the size and concentration of the NPs but the bactericidal mechanisms of Zn and ZnO NPs still are unknown. Recently, ZnO NPs have begun to be used in food packaging, although there is some concern about the potential impact of NPs on the health of consumers. According to some studies, ZnO NPs exhibit minimal toxicity to human cells.[20] Heng et al[21] demonstrated the cytotoxic effect of ZnO NPs on human bronchial epithelium cells, but the effect of ZnO NPs on other human cells has not been confirmed yet and additional research is needed. In addition, Ingle et al[22] has reported interesting data on the antimicrobial effect of Cu and CuO NPs. Das et al[23] demonstrated that nanostructured Cu efficiently inhibits the growth of *S. mutans*, *E. coli*, and *B. subtilis*. Xu et al[24] studied the susceptibility of gram-positive and gram-negative bacteria to Cu NPs and found that gram-negative bacteria are more susceptible. Like other NPs, Cu NPs showed size-dependent bactericidal activity. Several in vivo and in vitro studies on the toxicity of Cu NPs to human cells showed that they can cause irreversible damage.[25–27]

The main aim of our study was to combine the strong antibacterial activity of ZnO and CuO NPs with that of Fe_2O_3. ZnO and CuO NPs showed the most antibacterial activity against various bacterial species, while Fe_2O_3 NPs showed the least toxicity.[17] The combination of the three metal oxide NPs formed a new nanostructured CuZnFe oxide NP, called a trimetal oxide NP. To our best knowledge, multi-metal oxide NPs are usually prepared using complicated methods.[28] In the present study, we report, for the first time, the synthesis of CuZnFe oxide NPs using inexpensive chemicals and very easy solution process to form good quality nanostructures for large-scale production. This composite NP has the potential to control a wider range of bacterial infections compared to single NP material. Although ZnO NPs are relatively less toxic to human cells than CuO NPs in aqueous solution, they tend to aggregate and form large flocculates that decrease their antibacterial activity.[29] The stability of ZnO NPs in aqueous media may be improved by combining them with Fe_2O_3 NPs. Fe_2O_3 may provide some magnetic properties to these NPs resulting in their use in several additional applications. We tested the antibacterial activities of the CuZnFe oxide NP against gram-negative *E. coli* and gram-positive *Enterococcus faecalis*. Bacteria are unlikely to develop resistance against this new NP because bacteria must go through a series of mutations to become resistant to the trimetal oxide NP. Therefore, this NP can combat existing and emerging bacterial infections.

Materials and methods

Synthesis of ZnO NPs

ZnO NPs were synthesized using zinc acetate dihydrate [$Zn(CH_3COO)_2 \cdot 2H_2O$] and n-propyl amine [$CH_3–(CH_2)_2–NH_2$], purchased from Sigma-Aldrich Corporation (St Louis, MO, USA) and used without further purification. In a typical experiment, ~20 mL of n-propyl amine and 0.3 M zinc acetate

dihydrate were dissolved in 100 mL of methanol (MeOH). The obtained solution was stirred for 30 min for complete dissolution. The pH of the solution, measured using an expandable ion analyzer (Cole Parmer, Vernon Hills, IL, USA), was 12.2. After complete dissolution, the mixture was transferred to a three-necked refluxing pot and refluxed at 65°C for 6 h. After 6 h, a white precipitate was observed in the double-necked refluxing pot. A specialized temperature controller measured and controlled the refluxing temperature. The white powder was washed several times with MeOH, ethanol (EtOH), and acetone and dried at room temperature in a glass Petri dish. The obtained powder was characterized by its structural and chemical properties.

Synthesis of CuO NPs

CuO NPs were synthesized using copper acetate hydrate [$Cu(CH_3{\bullet}COO)_2{\bullet}H_2O$], n-propyl amine [$CH_3–(CH_2)_2–NH_2$], and sodium hydroxide (NaOH), purchased from Sigma-Aldrich and used as received. In a typical experiment, 0.3 M of copper acetate hydrate and 20 mL of n-propyl amine were mixed in 100 mL of MeOH with constant stirring, after which the solution turned blue. NaOH (0.1 M) was mixed into the solution in steps and shaken each time to ensure complete mixing. After adding the NaOH, the pH of the solution, checked via a pH meter (Cole Parmer), was 12.01 because of the increased basicity of the solution. The solution was transferred to a double-necked refluxing pot and refluxed at ~90°C for 6 h. As the temperature of the solution increased, the color changed from blue to dark brown to black. After the reaction was complete, the product was centrifuged at 3,000 rpm for 3 min and washed repeatedly with MeOH, EtOH, and acetone to remove the intermediate by-products. The material was dried at room temperature in a glass Petri dish and utilized for further chemical, morphological, and biological studies.

Formation of CuZnFe oxide NPs

Trimetal CuZnFe oxide NPs were formed by dissolving 0.3 M of zinc acetate dihydrate [$Zn(CH_3COO)_2{\cdot}2H_2O$], 0.3 M of copper acetate hydrate [$Cu(CH_3COO)_2{\cdot}H_2O$], and 0.3 M of iron nitrate nonahydrate [$Fe(NO_3)_3{\cdot}9H_2O$] in 300 mL of MeOH and stirring constantly for 30–40 min. When the solution was completely dissolved, 60 mL of n-propyl amine [$CH_3–(CH_2)_2–NH_2$] was added, followed by the dropwise addition of 0.1 M of NaOH to increase the basicity of the solution. The pH of the solution, checked via a pH meter (Cole Parmer), was 12.61. The mixture was transferred to a double-necked refluxing pot and refluxed at ~90°C for 6 h to obtain a red precipitate. The precipitate was washed several times with MeOH, EtOH, and acetone to remove ionic impurities and dried at room temperature. The material was studied for its structural and chemical properties.

Characterization of NPs

The phase, crystallinity, and size of the prepared nanostructures were characterized by their x-ray diffraction (XRD) pattern (Rigaku, Tokyo, Japan) obtained with $Cu_{K\alpha}$ radiation (λ=1.54178 Å) in the 20°–80° range at a scan speed of 6°/min, an accelerating voltage of 40 kV, and current of 40 mA. The morphology of the prepared nanostructures was analyzed using transmission electron microscopy (TEM, 200 kV; Hitachi, Tokyo, Japan). For TEM analysis of the nanostructures, NP powder was sonicated in EtOH for 10–20 min. Then a C-coated Cu grid (400 mesh) was dipped into the solution and dried at room temperature for morphological analysis.

In vitro experimental procedures

For the gram-positive bacterium, we chose *E. faecalis* because it can cause life-threatening infections in humans and shows a high level of resistance to antibiotics. In addition, *E. faecalis* has been found to be associated with up to 90% of the cases of chronic infection in teeth that underwent root canal treatment. For the gram-negative and facultative anaerobic bacterium, we chose *E. coli*, which can cause serious food poisoning and is occasionally responsible for food contamination.

Cell death analysis

The method used to measure bacterial cell death was previously described.[30,31] Briefly, cell death of *E. faecalis* and *E. coli* was analyzed using fresh culture grown in 25 mL of nutrient broth (NB; yeast extract 2 g/l, peptone 5 g/l, NaCl 5 g/l) in a 50-mL conical flask until the stationary phase showed no cell growth. The density of *E. faecalis* and *E. coli* was measured using an Eppendorf BioPhotometer Plus spectrophotometer (Thomas Scientific, Swedesboro, NJ, USA). A portion (5 mL) of the culture was transferred to a new sterile 20 mL conical flask. The bacteria were then added to three conical flasks containing Zn, Cu, and CuZnFe oxide NPs at 150 µg/mL and to three control flasks that did not contain any NPs. The flasks were then placed in a shaking incubator and shaken at 220 rpm for 5 h at 37°C, after which 1 mL from each flask was used to measure the optical density at 595 nm. The blank flasks contained 150 µg/mL of the corresponding NPs and media. The average of three readings was used for each NP.

Biofilm formation

The aim of this part was to test the ability of the bacteria *E. faecalis* and *E. coli* to form a biofilm in the presence of CuO, ZnO, and CuZnFe oxide NPs. Microbial biofilm is the main method of overcoming a harsh environment and the host immune system.[30] We used the spectrophotometric assay method to study biofilm formation. The bacteria were grown in a 96-well plate in triplicate using NB. Each well contained either NB with no NPs or NB with ZnO, CuO, or CuZnFe oxide NPs at 150 µg/mL. The plate was then incubated at 37°C for 48 h after being tightly sealed to prevent dehydration. The media in the plate were then poured into a designated waste container with 10% bleach. The plate was submerged in water to eliminate any excess media and was left to air dry. One-hundred twenty-five microliters of 0.1% crystal violet solution was added to each well and the plate was incubated at room temperature for 10 min. The crystal violet solution was poured into the designated waste container. The plate was submerged in water to eliminate any excess solution and left to air dry. Next, 200 µL of 100% EtOH was added to each well and the plate was incubated at room temperature for 15 min. EtOH in each well was mixed by pipetting gently to evenly distribute the color. The plate was then read in a Synergy™ HT Multi-Mode microplate reader (BioTek, Winooski, VT, USA) at λ=490 nm.

CFU/mL analysis

To test the ability of *E. faecalis* and *E. coli* to grow in the presence of the NPs, a viable cell count per milliliter was conducted using the colony-forming unit (CFU)/mL method. Bacterial cells (1 mL), grown overnight in 20 mL of NB (grown in a sterile 50 mL conical flask) and standardized to 1×10^5 cells, were mixed with 150 µg of ZnO, CuO, and CuZnFe oxide NPs and then the mixture was added to 9 mL of sterile distilled water. The solution underwent serial dilution until a dilution of 1×10^{-7} was obtained. NP-exposed samples and a control were streaked on four NB Petri dish plates each. The plates were then incubated overnight at 37°C. Each sample was tested in triplicate and the average of the three results was used.

Statistical analysis

To compare the quantitative variables of the groups, we used the nonparametric Mann–Whitney test; $p<0.05$ was considered statistically significant.

Results

Characterization of CuZnFe oxide NPs

We used the XRD pattern, shown in Figure 1, to characterize the size, phase, and crystalline character of CuZnFe, ZnO, and CuO NPs. Comparison of the XRD patterns, in Figure 1, to the XRD patterns of the materials in the International

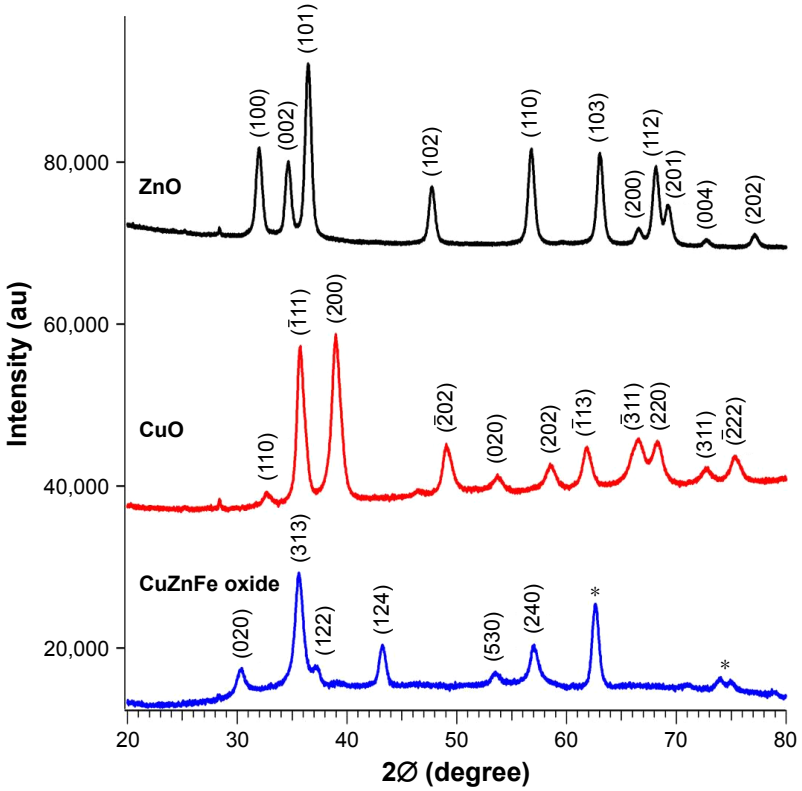

Figure 1 X-ray diffraction spectra of ZnO, CuO, and CuZnFe oxide nanoparticles. *Indicates that the peak is unidentified.

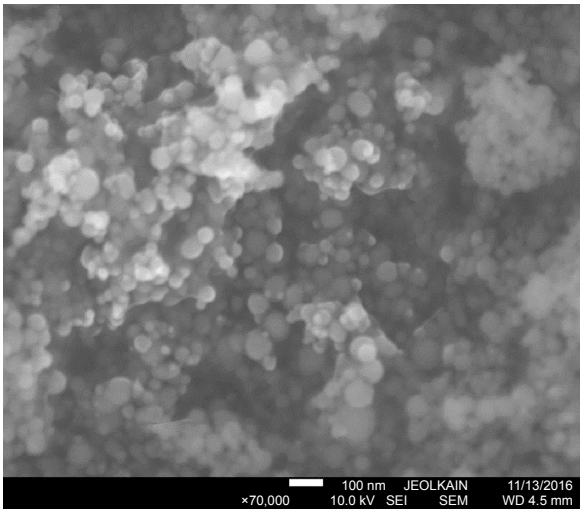

Figure 2 Scanning electron micrograph of the CuZnFe oxide nanoparticles.

Center for Diffraction Data identified our ZnO (black line), CuO (red line), and the trimetal CuZnFe oxide NPs (blue line) as ZnO (JCPDS card No 36–1451), CuO (JCPDS card No 05–066), and trimetal CuZnFe oxide (JCPDS card No 07–0392), respectively. However, three unidentified peaks were observed on the XRD spectrum of the CuZnFe oxide NPs. These peaks can be attributed to the complex formation of nanostructures in the mixed composite. The size of the crystallite can be calculated from XRD spectra using the Scherrer formula; $D = k\lambda/\beta\cos\theta$. The average size of the crystallite of the CuZnFe oxide NPs was calculated to be 23 nm, where k=0.9, λ=0.1541, and β is the full width at half-maximum of the peak at θ.

The morphology of the CuZnFe oxide NPs was characterized using scanning electron microscopy (SEM) and high-resolution TEM (HRTEM). Representative images from SEM and HRTEM are shown in Figures 2 and 3, respectively. The CuZnFe oxide NPs are almost spherical and have a clear tendency to agglomerate, which is normal for NPs because of the strong interparticle interaction induced by high surface energy. The size of agglomerate was analyzed by dynamic light scattering (Zeta Nanosizer) and found to be in 128 nm range. The average size of CuZnFe oxide NPs, based on several HRTEM images taken at different angles, was estimated to be 42±2 nm, whereas the average particle size based on XRD measurements was 19 nm smaller. The smaller size may be the result of the nanostructures merging together to form a larger molecule of mixed nanostructures. This is indicative of the presence of particle agglomeration, which is clarified by the HRTEM images of lattice fringes (Figure 3). The XRD calculation represents only the average single particle dimension for the bulk/powder nanostructures. The nanostructures were further assessed using energy dispersive x-ray spectroscopy (EDX), which is usually employed to map NPs based on their composition. Figure 4 shows the EDX spectrum of the mixed CuZnFe oxide NPs. The spectral peaks correspond to Zn Cu, Fe, and O, confirming the presence of elemental Zn, Cu, and ferrite, with O, in the NPs. No other impurity related to other elements was exhibited in the spectrum, which further shows that the synthesized nanostructures were only the mixed metal oxide nanostructures used.

Antibacterial activity of CuZnFe oxide NPs

Metallic NPs like Ag, Cu, Au, Ti, and Zn have proven effective against a wide range of bacterial species. Zn and Cu are widely used to combat microbial infections and have shown relatively less cytotoxicity.[32] The size of NPs allows them to penetrate the cell wall of bacteria and interact with cellular elements.[33] Therefore, the size of NPs may contribute to their bactericidal effect. The combination of the three metal oxides in the CuZnFe oxide NPs may enhance the therapeutic abilities of the NPs against a wide range of microbial infections.

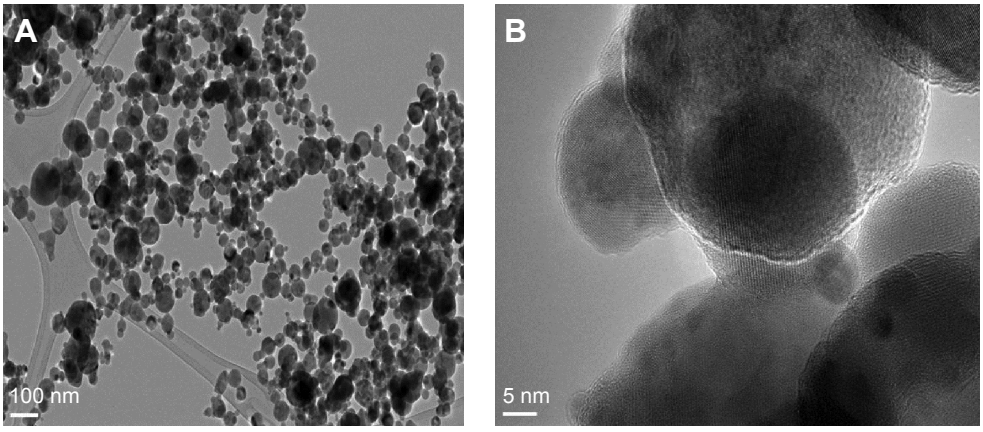

Figure 3 (**A**) High-resolution transmission electron microscope micrograph of the mixed CuZnFe oxide nanoparticles (NPs). (**B**) Atomic resolution of mixed CuZnFe oxide NPs.

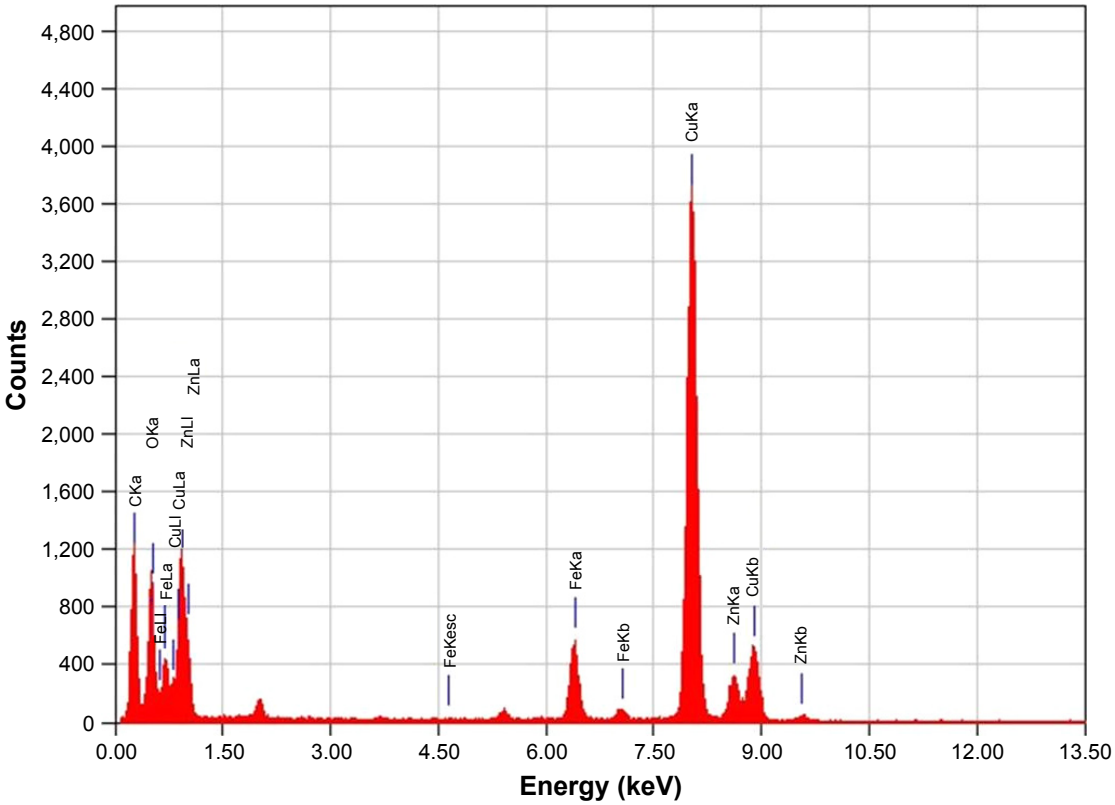

Figure 4 Energy dispersive x-ray spectroscopy spectrum of mixed CuZnFe oxide nanoparticles.

Figure 5 compares the bactericidal effect of the trimetal (CuZnFe) oxide NPs used in this study with that of pure ZnO and CuO NPs. The effect of FeO NPs against the bacterial cells was not investigated in this study. FeO NP has been proven to have a low or no toxic effect on different bacterial species, in particular *E. coli*.[17] The minimum concentration needed for the metal oxides to have a bactericidal effect on both bacterial species was at 150 µg/mL. The cells not exposed to NPs showed no drop in cell density after 5 h of incubation, while cells exposed to NPs showed a significant drop in cell density, except *E. coli* (gram-negative) exposed to CuO, where there was no cell death recorded. However, *E. coli* showed a 55% drop in cell density with exposure to ZnO and a nearly 85% drop in cell density with exposure to CuZnFe oxide NPs. *E. faecalis* (gram-positive) had the greatest drop in cell density when exposed to CuO NPs, with an ~59% drop in live cells compared to an ~25% drop in live cells with ZnO exposure and a 55% drop with exposure to trimetal (CuZnFe) oxide NPs.

The effect of trimetal (CuZnFe) oxide NPs on biofilm formation by both bacteria was proved, as shown in Figure 6. However, CuZnFe oxide NPs had the least effect on biofilm formation when compared to that of ZnO and CuO. There was an ~50% reduction in biofilm formation by *E. coli* in the presence of CuZnFe oxide NPs, while the presence of ZnO and CuO NPs caused an ~65% drop in biofilm formation by *E. coli* compared to control group. *E. faecalis* showed only a 26% drop in biofilm formation in the plate containing CuZnFe oxide NPs but a 62% and 40% drop in biofilm formation with ZnO and CuO NPs, respectively.

The growth of *E. faecalis* and *E. coli* on a nutrient agar was observed directly using a light microscope (Figure 7). This method is a useful and simple way to observe overnight growth of microbes without the presence of NPs or with 150 µg/mL of ZnO, CuO, or CuZnFe oxide NPs, and their effect on the CFU/mL count. Figure 8 presents the measurements of CFUs, indicating the antibacterial activity of CuZnFe oxide NPs. The viability of *E. faecalis* and *E. coli* was reduced by 40% and 38%, respectively, in the presence of CuZnFe oxide NPs. However, CuO NPs had almost no effect on *E. coli*, whereas they reduced the viability of *E. faecalis* by 70%. *E. faecalis* and *E. coli* showed a decrease in cell viability of 22% and 75%, respectively, after being exposed to ZnO NPs.

Discussion

Trimetallic nanoparticles were successfully synthesized by combining ZnO and CuO NPs with that of Fe_2O_3.

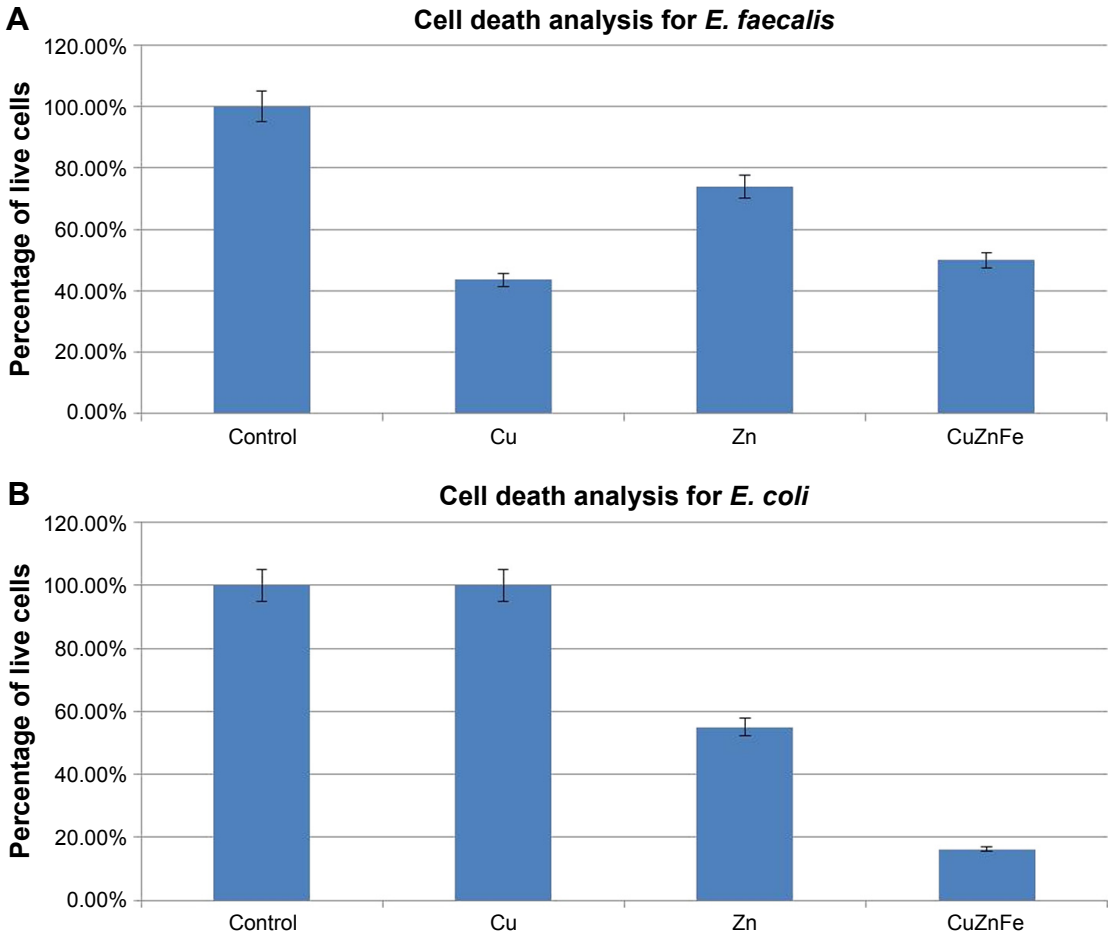

Figure 5 Percentage of live (**A**) *Enterococcus faecalis* (*E. faecalis*) cells and (**B**) *Escherichia coli* (*E. coli*) cells after 5 h of exposure to 150 µg/mL of metal oxide nanoparticles. Cells were grown in nutrient broth.

The combination of the three metal oxide NPs formed a new nanostructured CuZnFe oxide NP. In the present study, we used inexpensive chemicals and a very easy process for fabrication of high-quality trimetal (CuZnFe) oxide NPs. Multimetal oxide NPs are usually prepared using complicated methods. Based on the synthesis of CuZnFe oxide NPs, the use of metal salt of acetate and amine, in the current study, was due to that the acetate and amine can be easily dissociated in solution due to the breaking of hydrogen bonds at the time of refluxing of solution resulting in reaction with the other metal compound. This will easily react with the metal acetate ($MCH_3COO–$) group initially. In solution, the metal ions ($M=Cu^{2+}$, $Fe^{2/3+}$ and Zn^{2+} ions) react with n-propyl-amine group to form a metal complex ($MN–(CH_2)_2–CH_3$). When the refluxing temperatures increase, the hydroxyl (OH^-) ions from the used solvent methanol react with this metal complex and the metal ions from the complex decomposes, and then react to the hydroxyl (OH^-) ions to form metal hydroxide [$M(OH)_2$]. At higher refluxing temperature, hydroxide molecules change into metal oxide and water molecules. The by-products of the reaction [$(CH_3)_2N–(CH_2)_2–CH_3$, CH_3COOH and water molecule] were leached out during centrifugation of the product.[34,35]

Antibacterial activities of CuZnFe oxide NPs were tested against gram-negative *E. coli* and gram-positive *E. faecalis*. CuZnFe oxide NPs had an effect on both bacterial cells by reducing their viability and their ability to synthesize biofilm. Over the last few decades, bacterial resistance has challenged scientists to develop novel antimicrobial agents. Among them, metal NPs have shown strong antibacterial activity in several studies.[2,3,9] Importantly, it is hypothesized that metal NPs might have the potential to control bacterial resistance because NPs target multiple biomolecules at once.[8,9] However, the effect of metal oxide NPs on bacterial growth varies widely among bacterial species and even among strains of the same species.[7,17,20] Based on the cell wall structure, bacterial cells can be divided into two distinct types: gram-positive and gram-negative. Gram-positive bacteria have a thicker layer of peptidoglycan in their cell wall than that of gram-negative bacteria. However, gram-negative bacteria

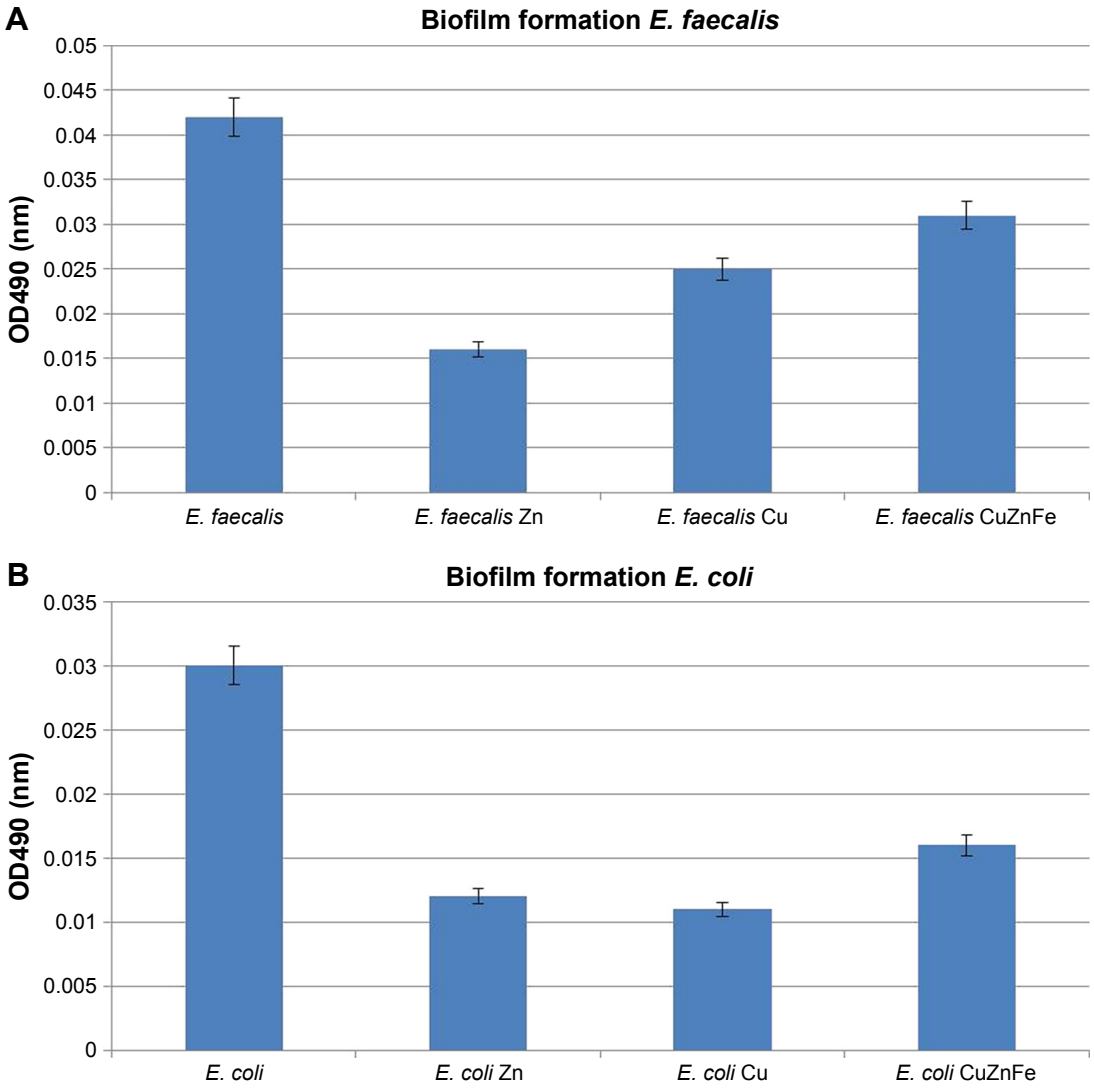

Figure 6 Ability of (**A**) *Enterococcus faecalis* (*E. faecalis*) and (**B**) *Escherichia coli* (*E. coli*) in nutrient broth to form biofilm after incubation with 150 μg/mL of metal nanoparticles as demonstrated by absorbance at 490 nm wavelength in a spectrophotometric reading.

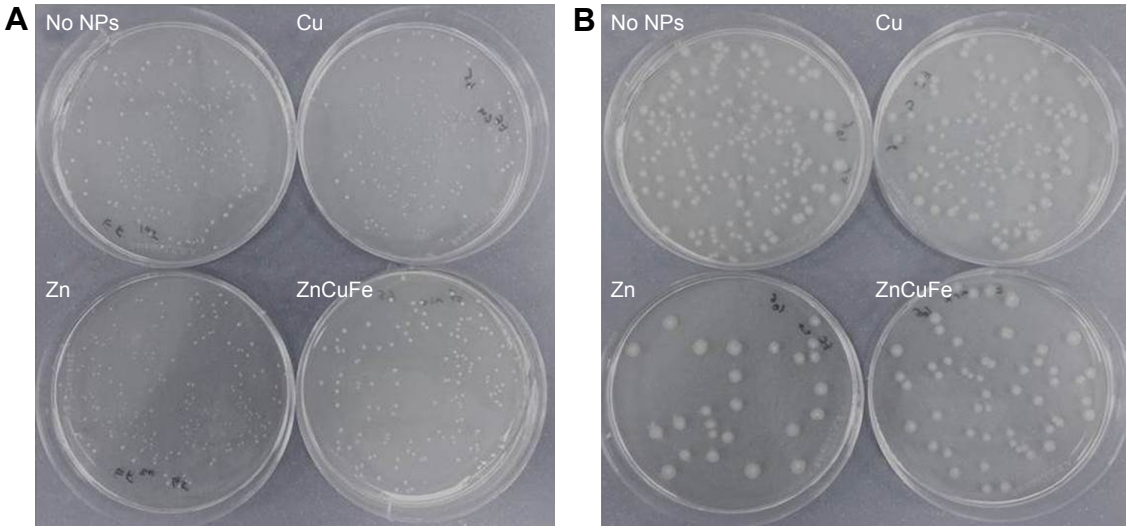

Figure 7 Representative images of overnight growth of microbes on nutrient agar with no nanoparticles (NPs) or with 150 μg/mL of ZnO, CuO, or CuZnFe oxide NPs and their effect on the colony-forming unit/mL count: (**A**) *Enterococcus faecalis*, (**B**) *Escherichia coli*.

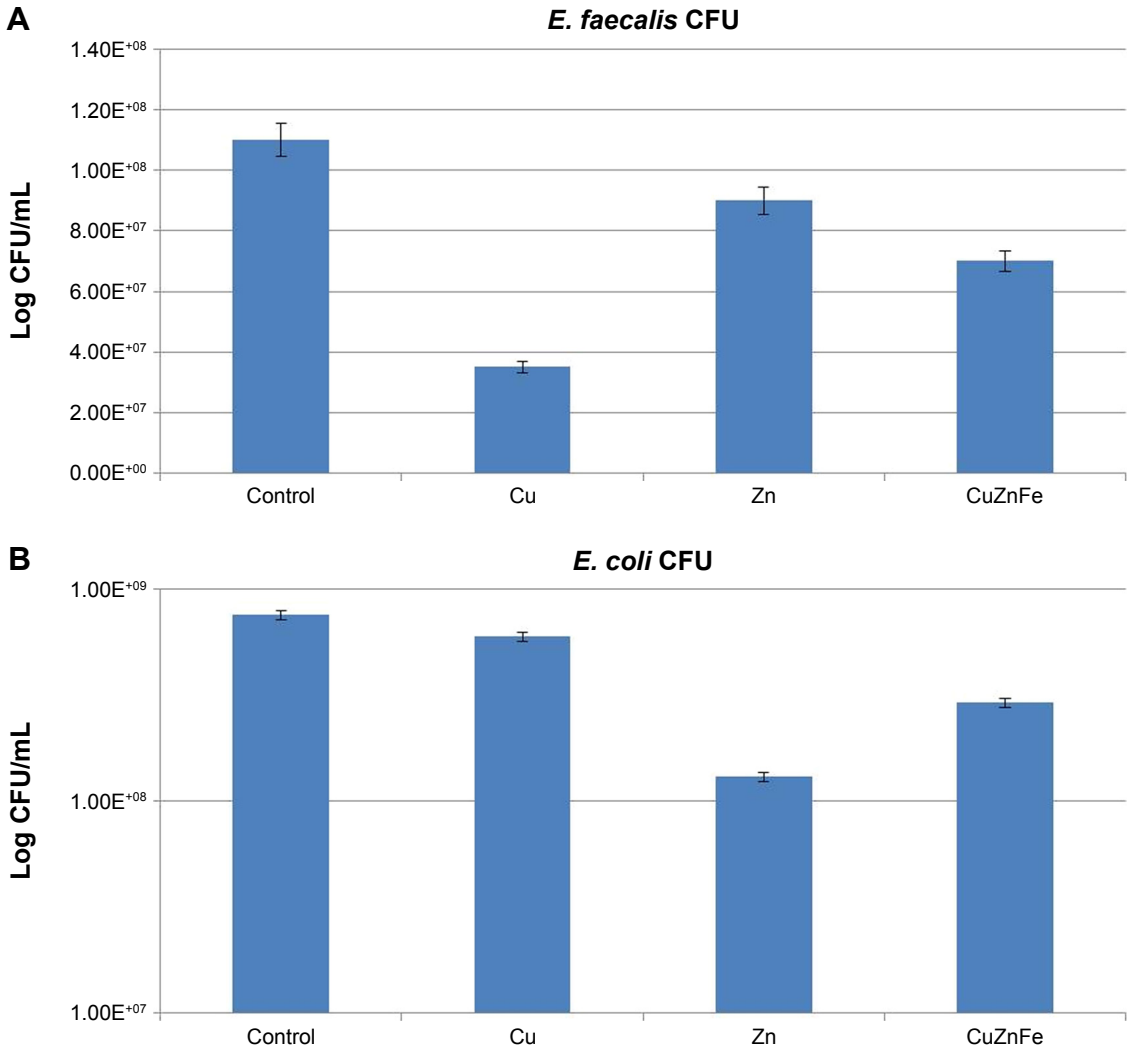

Figure 8 Colony-forming units (CFU) for (**A**) *Enterococcus faecalis* (*E. faecalis*) and (**B**) *Escherichia coli* (*E. coli*) after incubation in nutrient broth overnight with no nanoparticles (NPs) or in the presence of 150 μg/mL of metal oxides NPs.

possess an additional outer membrane constructed mainly of negatively charged lipopolysaccharide molecules (LP).

In the present study, we observed that CuZnFe oxide NPs have detrimental effects on *E. coli* (gram-negative) compared to the effects caused by individual CuO and ZnO NPs. CuZnFe oxide NPs were also found to be more bactericidal than ZnO against *E. faecalis* (gram-positive), but 7% lower than CuO NPs. CuZnFe oxide NPs in this study form agglomerates with an average size of ~128 nm. It seems that these large agglomerates are less likely to pass through the cell wall to cause bacterial damage from the interior, and thus penetration is unlikely the main mechanism for antibacterial activity of CuZnFe oxide NPs. But it can slowly release metal ions capable of crossing into membranes and disrupt cellular processes from inside the cell.[12,29] Another potential mechanism that might explain susceptibility of *E. coli* to CuZnFe oxide NPs is its higher affinity to LP,[36] the main constituent of the outer membrane of gram-negative bacteria. The physical interaction between CuZnFe oxide NPs and bacterial cells can disrupt the cell wall structure, leading to malfunction and to finally bacterial death. Thus, a bactericidal activity of trimetal oxide NPs can be attributed to a variety of properties. We assumed that CuZnFe oxide NPs are characterized differently from individual metal NPs due to their size and surface chemistry. The exact mechanisms for antibacterial activity of CuZnFe oxide NPs are still unclear and more investigation is required.

The individual CuO NPs had a greater impact on *E. faecalis* than on *E. coli* as assessed by cell death analysis (Figure 5). This is consistent with the findings of Ruparelia et al,[7] who also reported that CuO NPs affect various strains of *E. coli* differently. In this matter, they concluded that gram-negative bacteria may be affected less by the CuO NPs, which might involve more complex mechanisms. Also, Premanathan et al[37] found that gram-negative bacteria can be more resistant to CuO NPs than gram-positive bacteria. Of the different metals,

Cu and CuO have been widely used as cheap and effective bacteriostatic agents for sterilizing liquids and biological tissues.[32] It is important to note that some bacterial species are more sensitive to particular NPs than are others.[26,32] Therefore, CuO NP may be a promising antibacterial agent in combination with other metallic NPs. By contrast, we used ZnO NPs and showed a greater effect on the viability of the gram-negative *E. coli* than on the gram-positive *E. faecalis*, a result that may correspond to the thickness of the cell walls.

The results of CFU measurements indicated that the action of CuZnFe oxide NPs on *E. coli* was non-permanent, by showing recovery of the treated cells (Figure 8). The CFU results also indicated that the CuZnFe oxide NPs had a similar effect on *E. coli* and *E. faecalis* and an intermediate effect compared to the effects by the CuO or ZnO NPs. Trimetal (CuZnFe) oxide NPs affected biofilm formation to a lesser degree than did individual ZnO and CuO NPs. This indicates that the reduction in biofilm formation was not a result of cell loss but of the NP effect. Reduced biofilm formation with exposure to CuO and ZnO correlated with cell death and reduced CFU count for both *E. faecalis* and *E. coli*, but this was not the case with CuZnFe oxide NPs. The reduced disruption of biofilm formation by CuZnFe oxide NPs might result from the disruption in quorum sensing rather than from the effect of NPs. Quorum sensing has been established as an important factor in biofilm formation in both gram-positive and gram-negative bacteria.[38–41] However, more investigation is needed on the effect of metallic NPs on biofilm inhibition to fully understand the reason. Also, there is a need to know how biofilm inhibition occurs and what antibacterial mechanisms are involved.

To sum up, the implication from the results of our study is that trimetal (CuZnFe) oxide NPs can be very useful in terms of antibacterial activity. Overall, the effect of CuZnFe oxide NPs on *E. faecalis* and *E. coli* lies between the effect of CuO and ZnO NPs. Therefore, we assume that the cytotoxicity of CuZnFe oxide NPs may be also between that of pure ZnO and CuO nanoparticles. This might be explained by the buffering caused by the presence of ferric oxide (Fe_2O_3) in the trimetal NPs, leading to a reduced toxic effect. Also, it has to be emphasized that the presence of Fe_2O_3 NPs causes less toxicity than other metal oxide NPs, as previously suggested by Azam et al.[17] However, further investigations are needed to determine whether these hypotheses are true or not. Finally, with the current drug-delivery techniques, CuZnFe oxide NPs could be administered to the infected site for in situ treatment. These NPs could also be used as coating agents for various medical devices to prevent attachment and growth of a wide range of pathogenic bacteria.

Conclusion

The antimicrobial effect of the trimetal (CuZnFe) oxide NPs on both gram-positive and gram-negative bacteria was studied and compared with that of ZnO and CuO NPs. The CuZnFe oxide NPs were characterized using XRD, HRTEM, and EDX. HRTEM images showed that the NPs are almost spherical with a tendency to agglomerate. On the basis of several HRTEM images taken at different angles, the average particle size of CuZnFe oxide NPs was estimated to be 42±2 nm. Analysis of *E. coli* cell death demonstrated that CuZnFe oxide NPs have greater antibacterial efficiency than pure ZnO and CuO NPs. On the other hand, the effect of CuZnFe oxide NPs on *E. faecalis* was between that of ZnO and CuO. The monitoring of biofilm formation by both bacterial cells in the presence of the NPs used in these experiments revealed that the efficiency of CuZnFe oxide NPs in inhibiting biofilm formation is comparable to that of pure ZnO and CuO NPs. However, the number of CFUs showed that the effect of CuZnFe oxide NPs on cell viability was between that of the ZnO and CuO NPs.

Acknowledgments

This work was supported by King Saud University, Deanship of Scientific Research, College of Science Research Center, Kingdom of Saudi Arabia.

Author contributions

KEA, HSA, and AAN designed the study and the experiments, and wrote the manuscript. HSA and AAN carried out the biological part of the experiments. KEA, RW, AMA, and AME synthesized and characterized the NPs. All authors helped discuss, interpret, and shape the research and the manuscript, contributed toward data analysis, drafting and critically revising the paper, gave final approval of the version to be published, and agree to be accountable for all aspects of the work.

Disclosure

The authors report no conflicts of interest in this work.

References

1. Ventola CL. The antibiotic resistance crisis: part 1: causes and threats. *P T*. 2015;40(4):277–283.
2. Alanis AJ. Resistance to antibiotics: are we in the post-antibiotic era? *Arch Med Res*. 2005;36(6):697–705.
3. Davies J, Davies D. Origins and evolution of antibiotic resistance. *Microbiol Mol Biol Rev*. 2010;74(3):417–433.
4. Riley MA, Robinson SM, Roy CM, Dennis M, Liu V, Dorit RL. Resistance is futile: the bacteriocin model for addressing the antibiotic resistance challenge. *Biochem Soc Trans*. 2012;40(6):1438–1442.

5. Bjarnsholt T. The role of bacterial biofilms in chronic infections. *APMIS Suppl*. 2013;121(Suppl s136):1–58.
6. Shen Y, Zhao J, de la Fuente-núñez C, et al. Experimental and theoretical investigation of multispecies oral biofilm resistance to chlorhexidine treatment. *Sci Rep*. 2016;6:27537.
7. Ruparelia JP, Chatterjee AK, Duttagupta SP, Mukherji S. Strain specificity in antimicrobial activity of silver and copper nanoparticles. *Acta Biomater*. 2008;4(3):707–716.
8. Jiang W, Mashayekhi H, Xing B. Bacterial toxicity comparison between nano- and micro-scaled oxide particles. *Environ Pollut*. 2009; 157(5):1619–1625.
9. Dizaj SM, Lotfipour F, Barzegar-Jalali M, Zarrintan MH, Adibkia K. Antimicrobial activity of the metals and metal oxide nanoparticles. *Mater Sci Eng C Mater Biol Appl*. 2014;44:278–284.
10. Gu H, Ho P, Tong E, Wang L, Xu B. Presenting vancomycin on nanoparticles to enhance antimicrobial activities. *Nano Lett*. 2003;3(9): 1261–1263.
11. Huang Z, Zheng X, Yan D, et al. Toxicological effect of ZnO nanoparticles based on bacteria. *Langmuir*. 2008;24(8):4140–4144.
12. Hayden SC, Zhao G, Saha K, et al. Aggregation and interaction of cationic nanoparticles on bacterial surfaces. *J Am Chem Soc*. 2012;134(16): 6920–6923.
13. Raghupathi KR, Koodali RT, Manna AC. Size-dependent bacterial growth inhibition and mechanism of antibacterial activity of zinc oxide nanoparticles. *Langmuir*. 2011;27(7):4020–4028.
14. Liu Y, He L, Mustapha A, Li H, Hu ZQ, Lin M. Antibacterial activities of zinc oxide nanoparticles against *Escherichia coli* O157:H7. *J Appl Microbiol*. 2009;107(4):1193–1201.
15. Shakerimoghaddam A, Ghaemi EA, Jamalli A. Zinc oxide nanoparticle reduced biofilm formation and antigen 43 expressions in uropathogenic *Escherichia coli*. *Iran J Basic Med Sci*. 2017;20(4):451–456.
16. Jones N, Ray B, Ranjit KT, Manna AC. Antibacterial activity of ZnO nanoparticle suspensions on a broad spectrum of microorganisms. *FEMS Microbiol Lett*. 2008;279(1):71–76.
17. Azam A, Ahmed AS, Oves M, Khan MS, Habib SS, Memic A. Antimicrobial activity of metal oxide nanoparticles against Gram-positive and Gram-negative bacteria: a comparative study. *Int J Nanomedicine*. 2012;7:6003.
18. Hernández-Sierra JF, Ruiz F, Cruz Pena DC, et al. The antimicrobial sensitivity of *Streptococcus mutans* to nanoparticles of silver, zinc oxide, and gold. *Nanomedicine*. 2008;4(3):237–240.
19. Fang M, Chen JH, Xu XL, Yang PH, Hildebrand HF. Antibacterial activities of inorganic agents on six bacteria associated with oral infections by two susceptibility tests. *Int J Antimicrob Agents*. 2006;27(6): 513–517.
20. Reddy KM, Feris K, Bell J, Wingett DG, Hanley C, Punnoose A. Selective toxicity of zinc oxide nanoparticles to prokaryotic and eukaryotic systems. *Appl Phys Lett*. 2007;90(21):213902–2139023.
21. Heng BC, Zhao X, Xiong S, Ng KW, Boey FY, Loo JS. Toxicity of zinc oxide (ZnO) nanoparticles on human bronchial epithelial cells (BEAS-2B) is accentuated by oxidative stress. *Food Chem Toxicol*. 2010;48(6): 1762–1766.
22. Ingle AP, Duran N, Rai M. Bioactivity, mechanism of action, and cytotoxicity of copper-based nanoparticles: a review. *Appl Microbiol Biotechnol*. 2014;98(3):1001–1009.
23. Das R, Gang S, Nath SS, Bhattacharjee R. Linoleic acid capped copper nanoparticles for antibacterial activity. *J Bionanosci*. 2010; 4(1–2):82–86.
24. Xu J, Ji W, Shen Z, et al. Preparation and characterization of CuO nanocrystals. *J Solid State Chem*. 1999;147(2):516–519.
25. Chen Z, Meng H, Xing G, et al. Acute toxicological effects of copper nanoparticles in vivo. *Toxicol Lett*. 2006;163(2):109–120.
26. Prabhu BM, Ali SF, Murdock RC, Hussain SM, Srivatsan M. Copper nanoparticles exert size and concentration dependent toxicity on somatosensory neurons of rat. *Nanotoxicology*. 2010;4(2):150–160.
27. Siddiqui MA, Alhadlaq HA, Ahmad J, Al-Khedhairy AA, Musarrat J, Ahamed M. Copper oxide nanoparticles induced mitochondria mediated apoptosis in human hepatocarcinoma cells. *PLoS One*. 2013; 8(8):e69534.
28. Shanthala V, Devi SS, Murugendrappa M. Synthesis, characterization and DC conductivity studies of polypyrrole/copper zinc iron oxide nanocomposites. *J Asian Ceramic Soc*. 2017;5(3):227–234.
29. Gordon T, Perlstein B, Houbara O, Felner I, Banin E, Margel S. Synthesis and characterization of zinc/iron oxide composite nanoparticles and their antibacterial properties. *Colloids Surf A*. 2011;374(1):1–8.
30. Costerton JW, Stewart PS, Greenberg EP. Bacterial biofilms: a common cause of persistent infections. *Science*. 1999;284(5418):1318–1322.
31. Das T, Manefield M. Pyocyanin promotes extracellular DNA release in *Pseudomonas aeruginosa*. *PLoS One*. 2012;7(10):e46718.
32. Ashfaq M, Verma N, Khan S. Copper/zinc bimetal nanoparticles-dispersed carbon nanofibers: a novel potential antibiotic material. *Mater Sci Eng C Mater Biol Appl*. 2016;59:938–947.
33. Ingle A, Gade A, Pierrat S, Sonnichsen C, Rai M. Mycosynthesis of silver nanoparticles using the fungus Fusarium acuminatum and its activity against some human pathogenic bacteria. *Curr Nanosci*. 2008; 4(2):141–144.
34. Wahab R, Khan F, Bing Yang Y, et al. Zinc oxide quantum dots: multifunctional candidates for arresting C2C12 cancer cells and their role towards caspase 3 and 7 genes. *RSC Adv*. 2016;6(31):26111–26120.
35. Wahab R, Siddiqui MA, Saquib Q, et al. ZnO nanoparticles induced oxidative stress and apoptosis in HepG2 and MCF-7 cancer cells and their antibacterial activity. *Colloids Surf B Biointerfaces*. 2014;117:267–276.
36. Zhang L, Jiang Y, Ding Y, Povey M, York D. Investigation into the antibacterial behaviour of suspensions of ZnO nanoparticles (ZnO nanofluids). *J Nanopart Res*. 2007;9(3):479–489.
37. Premanathan M, Karthikeyan K, Jeyasubramanian K, Manivannan G. Selective toxicity of ZnO nanoparticles toward Gram-positive bacteria and cancer cells by apoptosis through lipid peroxidation. *Nanomedicine*. 2011;7(2):184–192.
38. Cvitkovitch DG, Li YH, Ellen RP. Quorum sensing and biofilm formation in *Streptococcal* infections. *J Clin Invest*. 2003;112(11):1626.
39. Hentzer M, Riedel K, Rasmussen TB, et al. Inhibition of quorum sensing in *Pseudomonas aeruginosa* biofilm bacteria by a halogenated furanone compound. *Microbiology*. 2002;148(Pt 1):87–102.
40. Kong KF, Vuong C, Otto M. *Staphylococcus* quorum sensing in biofilm formation and infection. *Int J Med Microbiol*. 2006;296(2):133–139.
41. Mohamed JA, Huang W, Nallapareddy SR, Teng F, Murray BE. Influence of origin of isolates, especially endocarditis isolates, and various genes on biofilm formation by *Enterococcus faecalis*. *Infect Immun*. 2004; 72(6):3658–3663.